Carpathian Journal of Earth and Environmental Sciences, February 2021, Vol. 16, No. 1, p. 99 – 115; Doi:10.26471/cjees/2021/016/159

MICROSCOPIC "STRUCTURE-FROM-MOTION" PHOTOGRAMMETRY, A METHOD FOR MICROFOSSIL STUDY

Tony-Cristian DUMITRIU[1], Sergiu LOGHIN[1]*, Mihai BRÂNZILĂ[1], Dorin Sorin BACIU[1], Simina Dumitrița DUMITRIU[1], Silvia MARE[2], Ana Maria DUMITRIU[1] & Viorel IONESI[1]

[1]„Alexandru Ioan Cuza" University of Iași, Faculty of Geography and Geology, Department of Geology, Carol 1 Bd. 700505, Iași, Romania. tony.dumitriu@uaic.ro, vioion@uaic.ro, mib@uaic.ro, dsbaciu@gmail.com, loghin_sergiu@yahoo.com, anamaria.hutu@yahoo.com, siminadumitriu@gmail.com;
[2]S.C. Geologic Worldwide Services S.R.L. Bucharest silvia_mare@yahoo.com.
**corresponding author. loghin_sergiu@yahoo.com,*

Abstract: The microfossils taxonomy, apart from the recently and thoroughly studied molecular data is mostly based on the morphology of their external shape. Classical microfossil studies involve the usage of an optic microscope in order to identify the external morphological characters, followed by detailed examination using Scanning Electron Microscopy (SEM). In many cases, for an accurate determination of the specimen, correlation of the characters from its opposite sides is necessary. Using 2D images in the determination process is quite hard and often could lead to poor and insufficient information gathering. This study presents a new method for the microfossil representation. The method allows a more accurate measurement of the morphology of the specimens. The "Structure-from-Motion" Photogrammetry technique makes use of a very accessible methodology: SEM photos and photogrammetry software. The 3D models have been made for nine specimens of foraminifera, ostracods, radiolarians, ascidian spicules, and a dinoflagellate cysts. The variability of the studied specimens proves that this method can be successfully applied to almost all groups of microorganisms.

Keywords: "Structure-from-Motion" Photogrammetry, 3-D microfossils, foraminifers, ostracods, radiolarians, spicules

1. INTRODUCTION

The 3-D "digitization" for the surface of a fossil has become a standard method in the last decade in paleontological studies. This type of virtual reconstruction has enhanced fossils studies by providing the 3-D models which offer to palaeontologists a better flexibility and accuracy in observing the characters of the specimen. Moreover, using this method, online databases have been created, offering the possibility for archiving and distributing processed data (Smith & Strait, 2008; Belvedere et al., 2011).

One good example of using this method is the 3-D "digitization" of some extinct vertebrate skeletons, which allowed to the researchers the study of the biomechanical aspects such as locomotion and feeding habits. Moreover, the researchers also used the method to calculate the volume of the soft tissue for some extinct animals and other details like the size and location of the muscles (Hutchinson et al., 2005; Rybczynski et al., 2008; Gatesy et al., 2009; Sellers et al., 2009).

A well-known method for 3-D digitization of a studied specimen is the laser scanning. Laser scanners have many types and sizes depending on the level of detail and size of the studied object. Moreover, the laser scanners imply very high costs (Falkingham, 2012). An alternative for this type of 3-D digitization method can be the photogrammetry, namely "Structure-from-Motion" photogrammetry (Westoby et al., 2012; Iglhaut et al., 2019). This method uses photos obtained with any type of digital camera. Next, by calculating the camera position it generates a 3-D point cloud from which a 3-D model can be reconstructed. In palaeontology this method has been

successfully used in the study of dinosaurs and other large footprints (Bates et al., 2009).

Regarding the microfossil study, a digitization process was accomplished using computer tomography (Görög et al., 2012). Although this method provides good results, it implies very high costs, as well as laser scanning.

An alternative to computer tomography is the "Structure from Motion" photogrammetry method with SEM photos. Gontard et al., (2016) used this method to study a particle of $LiTi(PO_4)_3$. The authors tried an open source software known as VisualSFM and a freeware software known as 123D Catch. Eulitz & Reiss (2015) managed to reconstruct a section of about 5 X 5 X 5 mm of a rabbit's kidney in 3-D using the same software.

This method was also used by Wynn et al., (2015), who modelled one foraminifera using Autodesk's 123DCatch. The model showed the topography of only a part of the specimen, with low quality textures and without a possibility to execute measurements.

The accuracy of the 3-D reconstruction differs very much from one software to another and the resulting 3-D models can have a low quality due to software restrictions (Dumitriu, 2013).

2. MATERIALS AND METHODS

The present paper uses a series of techniques that allow the modelling of the entire fossil specimen, with high quality textures and measurement possibilities.

The method used to create the 3-D models for the microfossils specimens was the "Structure from Motion" Photogrammetry. Although several software applications can create 3-D models from photographs, only few of them allow a high accuracy and even fewer have the functions that enable the creation of a complete 3-D model. A trial version of Agisoft`s Photoscan, was used on a computer with a software that enabled us to have full control of the 3-D reconstruction at high resolution and any number of photos.

Before proceeding with the 3-D reconstruction we focused our attention on the accuracy of the Photoscan software. As it is shown by Sutton et al., (2017) in their overview on virtual palaeontology, photogrammetry is the only 3-D reconstruction technique that can be applied in a large variety of situations for subjects with very different sizes. For large scenes Juad et al., (2016) demonstrated that Photoscan has an accuracy of 3 to 4 cm for a 3-D reconstructed perimeter of about 13 km^2. A study done by Koppel Engineering, shows that Photoscan has an accuracy of 1.3 mm for a 3-D reconstructed metal cone with a diameter of 10 m. Both studies show that Photoscan has a very high accuracy in 3-D reconstruction and its calculation algorithms provide comparable result with laser scanning. Due to the fact that the Photoscan algorithm, and other "Structure from Motion" software algorithm, works by detecting and other "Structure from Motion" software algorithm, works by detecting and matching features from overlapping photos it can also be used with SEM photos. To test the accuracy of Photoscan reconstruction using SEM photos, 60 pictures of a pyrite sample have been taken and used to generate a 3-D model using the software functions (Plate 1). From the resulting 3-D model we have separated 2 regular geometric shapes: 1 tetrahedron and 1 parallelepiped (Fig. 1) and extracted the volumes for each one.

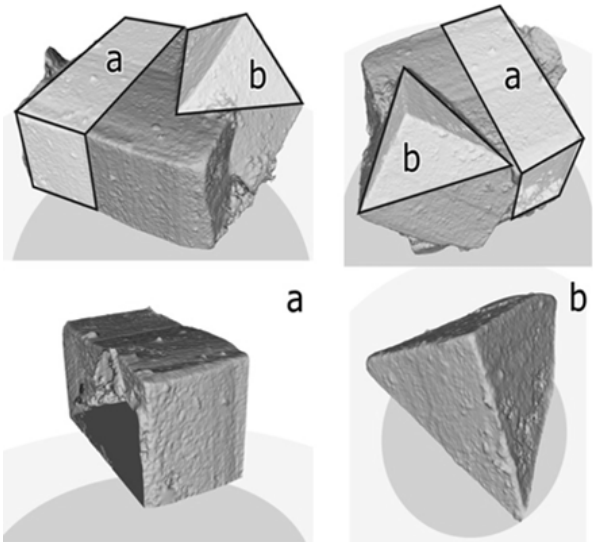

Figure 1. Pyrite sample reconstructed 3-D using SEM photos and Photoscan. Top images represent the whole sample, bottom images are separated regular geometric shapes.

Using the measurements taken directly from the SEM photos we reconstructed the same shapes in Sketchup (Fig. 2) and obtained another two volumes. The Photoscan volumes were almost identical to the ones created from direct measurements. The small difference between the two methods comes due to the fact that the 3-D reconstructed models have imperfect surfaces with complex irregular convex micro shapes, while the 3-D Sketchup models have no irregularities, their shape being mathematically created (Fig. 3).

The comparison between the volumes from the 3-D reconstruction and the ones from the 3-D Sketcup models shows a difference of about 10.61 % in volume for the tetrahedron and 11.7% for the parallelepiped shape (Table 1).

After testing the accuracy of the method several microfossils encompassing two foraminifers,

two ostracods, three radiolarians, one ascidian spicule and one dinoflagellate cyst (see plates 1 – 6) were prepared and photographed for the 3-D reconstruction process.

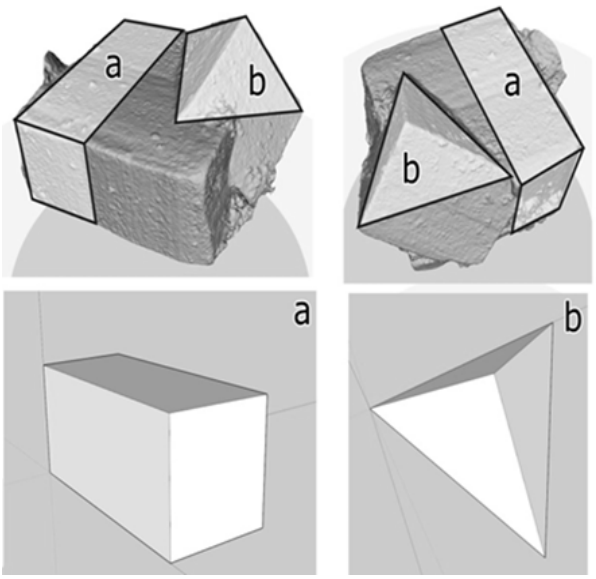

Figure 2. Pyrite sample reconstructed in 3-D using SEM photos and Photoscan in the top images and Sketchup in the bottom images.

In order to create a 3-D model for an entire microfossil, one set of overlapping 360° photos (Fig. 4) had to be created for each part of the specimen using a SEM microscope. The images where taken at an roughly 7° angle or a 14° angle depending on the characteristics of each modelled microfossil.

Table 1. Volume comparison between the 3-D models reconstructed with Photoscan ant the models reconstructed with Sketchup

	Tetrahedron	Parallelepiped
Volume SketchUP (μm^3)	14,556,130.00	96,985,000.00
Volume Photoscan (μm^3)	16,101,254.00	108,334,501.00
Volume difference (μm^3)	1,545,124.00	11,349,501.00
Volume Difference (%)	10.61	11.70

The resulting number of photos are 52 for each side for *Cycloforina karreri karreri*, 26 (each side) for *Quinqueloculina minakovae ukrainica*, 26 (each side) for *Cyprideis pannonica*, 52 (one side only) for *Loxoconcha minima*, two specimens *Amphisphaera coronata* with 26 photos for each side of the specimen, 52 photos (for one side only) *Podocyrtis (Podocyrtis) papalis*, 52 photos (one side only) *Spiniferites bentorii pannonicus* and 26 photos (one side only) for *Didemnum*–like spicule.

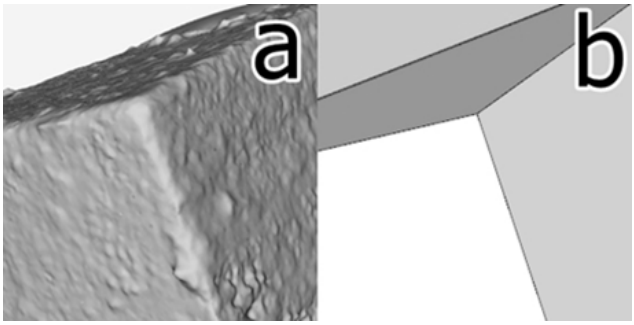

Figure 3. A corner of the tetrahedron (a-3-D model from Photoscan; b-3-D model from Sketchup) showing the difference in the surface shape.

The number of photos was decided depending on the morphology of the specimen surface. If the specimens had many ornamental features (ribs, spines, large and complicated pores) we have made sets of 52 pictures each side in order to create an accurate 3-D model of the fossil specimen.

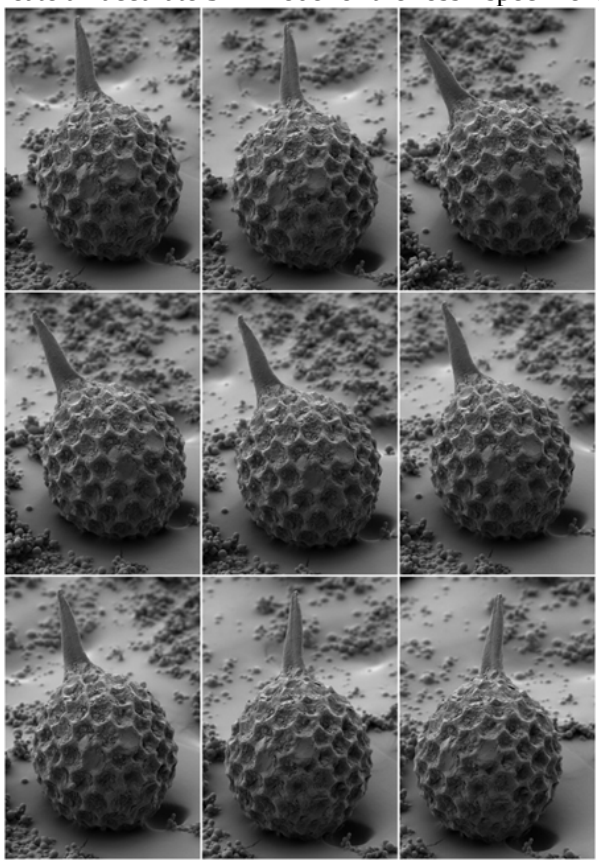

Figure 4. Eight overlapping photos from one set of *Amphisphaera coronata* (SEM photo).

To be able to turn the specimens on each side to be photographed we first mounted the fossil onto stand and glued it with carbon conductive tape (Fig. 5). For the other side of the specimen (another 360° set of photos) we had to dissolve the tape with acetone, detach the specimen, turn it on the other side and re-attach it on another carbon conductive tape.

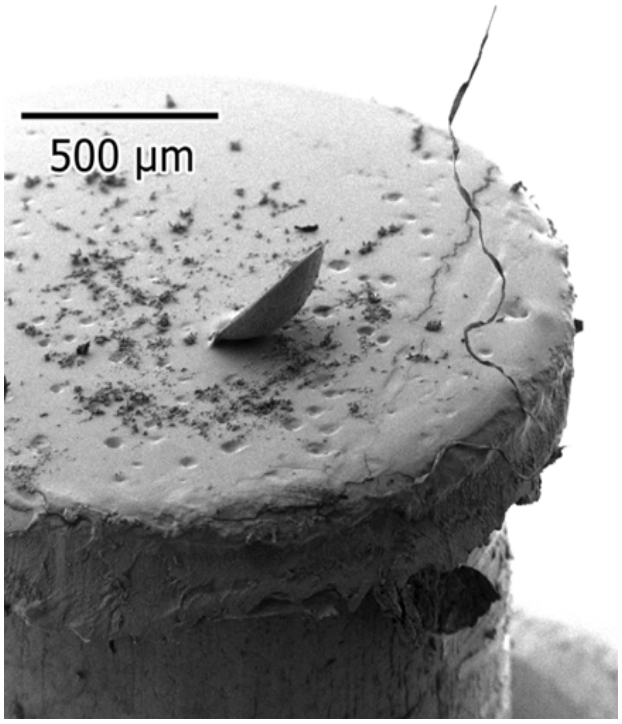

Figure 5. *Loxoconcha minima* glued with carbon conductive tape onto a stand (SEM photo).

The next step in obtaining the 3-D model for the microfossils was to process the photos and prepare them for the 3-D reconstruction by cropping them and readjusting the brightness, contrast and sharpness, depending on the Photoscan software returned results. Inside Photoscan the 3-D reconstruction process implies 4 main steps: photo alignment, dense cloud generation, mesh generation and texture generation.

Photo alignment is achieved by matching common points between each photo and finding the position of each photo in the 3-D space, which will generate a sparse point cloud that will be used in the dense point cloud generation process. Although in this first step the photos can be aligned automatically by the software, in some cases we had to assign some of the reference points manually. The manually introduced points, called markers (Fig. 6), helped the software to recognize common features between each photo and to generate the sparse point cloud.

The settings used for this step differ from specimen to specimen because they were used according to the results that the software generated. In general the "Accuracy" was set to "Medium" or higher, the "Pair preselection" was set to "Disabled" and "Key point" and "Tie point" limit set to zero.

The dense point cloud (Fig. 7) generation process has been achieved with the "Quality" setting set to "Medium" and "Depth filtering" set to "Mild".

The next step involved the mesh generation process (Fig. 8). We set the "Surface type" to "Arbitrary", the "Source data" to "Dense cloud", the "Face count" to 0 and "Interpolation" to "Enable (default)".

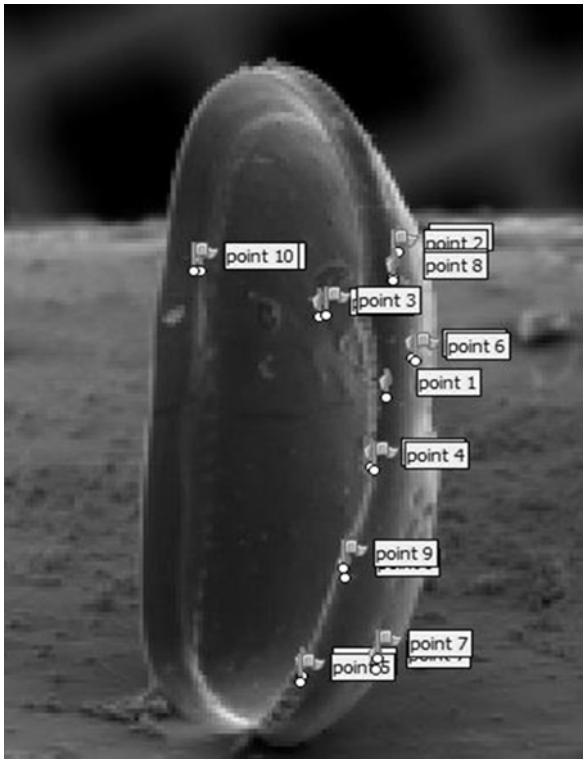

Figure 6. Markers used for reference in one photo from *Cyprideis pannonica* photo set (inside Photoscan).

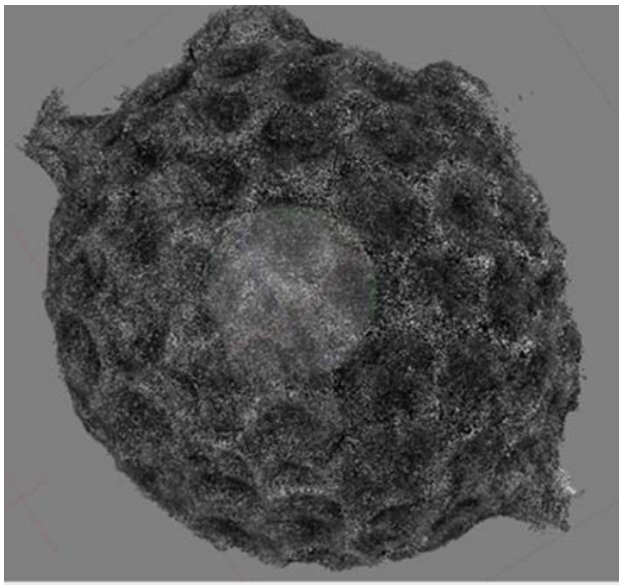

Figure 7. Dense point cloud of *Amphisphaera coronata* (inside Photoscan).

For the fourth step (texture generation – Fig. 9) we set the "Mapping mode" to "Generic", the "Blending mode" to "Mosaic (default)" and the "Texture size/count" to 16384/1.

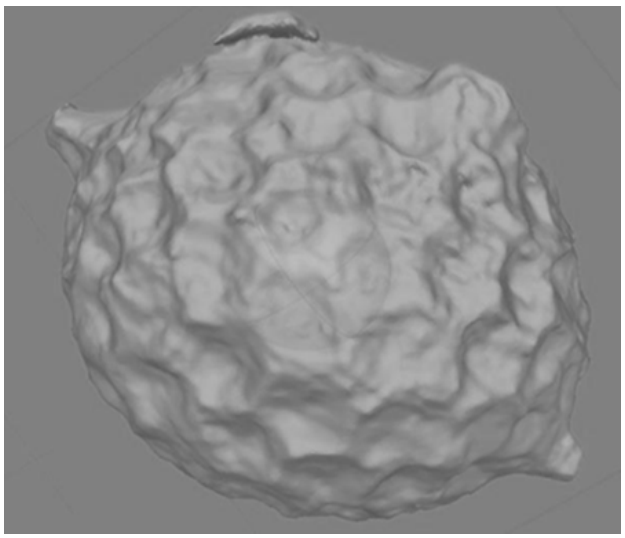

Figure 8. 3-D Mesh of *Amphisphaera coronata* (inside Photoscan).

All these four steps generated a rough textured 3-D model for the photographed part of the specimen.

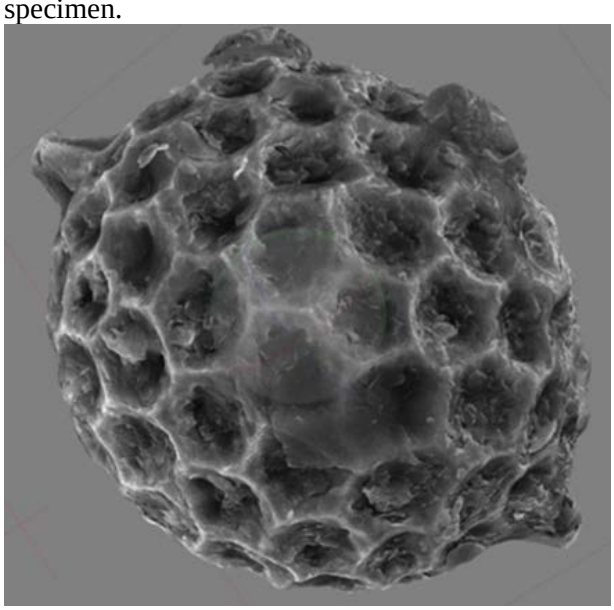

Figure 9. 3-D Mesh with textures of *Amphisphaera coronata* (inside Photoscan).

If the specimen was photographed only for one side, the model was cleaned by removing unwanted artefacts.

If the microfossil had 360° photos taken for both parts, then the process presented before had to be repeated for the second part and the two resulted 3-D models had to be stitched together using a few more steps. The first two steps implied manually assigning of corresponding makers for each half (Fig. 10) (named chunk in Photoscan) and aligning them using "Align chunks" function. In the next process the two aligned chunks, are glued together using "Merge chunks" function. After that the resulting chunk which contains the 3-D model for each side of the specimen had to be reprocessed using once more the "Build dense point cloud", "Build mesh" and "Build texture" functions.

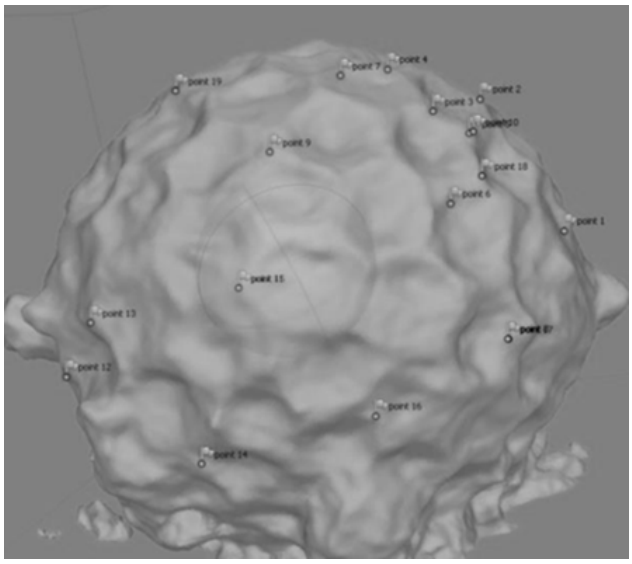

Figure 10. 3-D Mesh of one chunk with markers of *Amphisphaera coronata* (inside Photoscan).

3. RESULTS

After performing all these steps we obtained high quality textured 3-D models for each microfossil: plates 1-5 contain the 3-D models and therefore will be introduced only in the electronic version of the paper (see supplementary material).

3.1. Foraminifera

The taxonomy of the foraminifera is mostly based on the test morphology (Loeblich & Tappan, 1984, 1987), including the number and shape of the chambers, the chambers arrangement, the shape and position of the aperture and also the type of the ornamentation (Haynes, 1981). Moreover, each species may possess very distinctive test morphology. In this case the 3-D model provided very useful information for the foraminifera, which lead to a better determination of the species. The precise measurements of the length and width of the test, aperture, and tooth is very helpful in the species determination. Furthermore, based on the results obtained, several morphological variations have been also observed. Additionally, the width/length ratio was easily calculated, offering important information in the morphological study. The 3-D model also provide the possibility of a better comparison between fossils and recent specimens.

The 3-D modeled foraminifers are:

Genus *Cycloforina* Łuczkowska, 1972

Species Cycloforina karreri karreri (Reuss, 1869)

Description. The test is oval, elongated with

rounded periphery; tubular chambers, of almost uniform width; the surface of all chambers is covered with longitudinal ribs (Plates 2, 4), the number of which oscillates from seven to eight on the last chambers; sutures lines are distinct and deeply depressed. The aperture is circular with a thick rim, flush with the surface of the test and presents a short tooth, slightly visible. The length of the test is 360 μm while the width is 210 μm. The length/width ratio is 1.71.

The specimen (Fig. 11) was identified in a sample from the FH_3P_1 Rădăuți borehole, north-east Romania and it belongs to middle Miocene deposits (Dumitriu et al., 2018).

Figure 11. *Cycloforina karreri karreri* (SEM photo).

Despite the fact that there is no real replacement for an authentic fossil, there is still an incredibly important need to realize their digital preservation for a sustainable future development.

The reason is represented by the high importance and relevance of the holotypes, through which the digitization will facilitate the access of specialists for research purpose without the specimen to be affected by the constant handling. In other cases, i.e., museum collections the digitization process will allow the creation of the interactive database, available online, which will allow the access to different collections not only to the scientific personnel, but also to the public by free access to the virtual exhibition and for educational purposes.

Genus *Quinqueloculina* d'Orbigny, 1846, emend Łuczkowska, 1972

Species Quinqueloculina minakovae ukrainica (Didkowski, 1961)

Description. The test shape is oval to elongate, with the surface partially covered with poorly visible longitudinal slanting ribs at the periphery (Fig. 12). The middle chamber is slightly inflated. The aperture is elongated, medium sized, oval-elongated, with a short quadrate tooth, somewhat bifurcated, and a thick rim (Plates 2, 4). The length and the width of the test is 280 μm and 220 μm respectively. The ratio between the length and the width of the test is 1.27.

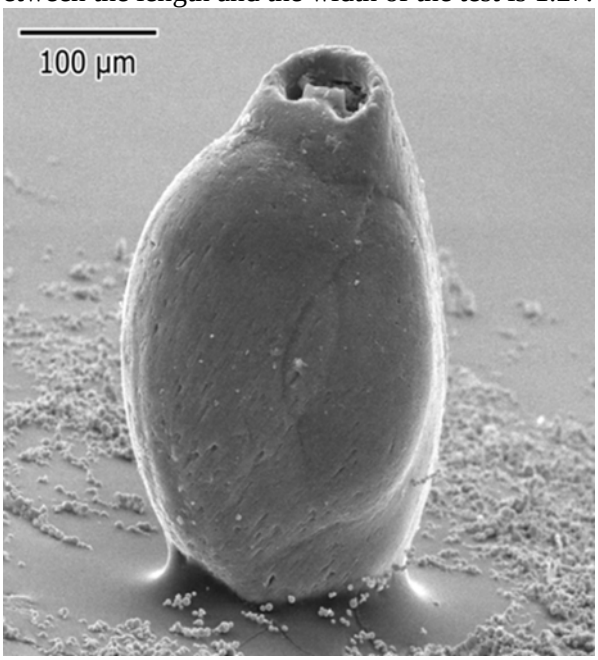

Figure 12. *Quinqueloculina minakovae ukrainica* (SEM photo).

3.2. Ostracods

The use of 3-D modelling for ostracods was very useful for the recognition of the characteristics of the species. Using the 3-D models of the ostracods specimens allowed us to observe the length/height ratio, the sexual dimorphism and also the precise position of some ornamentation elements (spines, tubercles, and hinge) on the surface of the carapace. The specimens of ostracods used for 3-D modelling are:

Genus *Cyprideis* Jones, 1857

Species *Cyprideis pannonica* (Méhes, 1908)

Description. The lateral outline has an oval form. The maximum height is slightly greater than the half of the length (Fig. 13). The dorsal margin is somewhat convex and the ventral margin is slightly concave in the anterior half. The anterior margin is well rounded, while the posterior end is obtusely rounded (see plates 2, 4). The maximum width is encountered in the posterior part. The surface of the valve is almost smooth, except for the normal pores

depressions and the almost concentrically pitted anterior, ventral and posterior ventral areas. The specimen presents 5 visible developed spines in the anterior margin and one spine placed in the posterior ventral. It also has four rows well pronounced muscle scars, with the fulchral point visible and a V shaped scar trough the anterior margin.

Figure 13. *Cyprideis pannonica* (SEM photo).

Figure 14. *Loxoconcha minima* (SEM photo).

This specimen has been collected from the Middle Miocene sediments outcroping in north-east Romania. The cytheracean ostracods (as *Cyprideis* genera) are indicatig a shallow, well oxygenated environment and water salinity varying from brackish to normal (van Morkoven 1963; Whatley, 1995).

Genus *Loxoconcha* Sars, 1866

Species *Loxoconcha minima* (Müller, 1894)

Description. The lateral outline of the carapace is rhomboidal-elongate. The anterior end is well rounded and the posterior end is upward rounded. The dorsal margin is straight, the ventral margin is slightly upper orientated trough the posterior area and rounded. The surface of the valve is almost smooth except for the concentrically arranged rows of pore depressions (Fig. 14). The muscle scars are disposed in a row of four adductor muscles and a V-shaped muscle towards the anterior margin (Plates 2, 5).

3.3. Radiolarians

The advantage of the 3-D reconstruction of the radiolarians (microorganisms) is that their study was easier and more accurate. This new imaging technique helped us understand the real shape of the species and therefore determine it much easier.

The species of radiolarians that we 3-D modelled are:

Genus *Podocyrtis* Ehrenberg, 1847

Species *Podocyrtis (Podocyrtis) papalis* Ehrenberg: Ling et al., 1991

Description. The cephalis is sub-hemispherical, with many small pores, bearing a horn of variable length, which is usually three-bladed and sometimes conical. The collar structure is marked by a change in contour. The thorax is inflated-conical, with circular pores in longitudinal rows separated by ribs. The lumbar structure is not (or only very slightly) expressed externally. The abdomen is inverted and truncate-conical, with pores and ribs similar to those of the thorax. The part of abdomen with pores is generally shorter than the thorax and this it is followed by a part with no pores from which arise three large, shovel-shaped, feet (Riedel & Sanfilippo, 1970).

This specimen (Fig. 15, Plates 3, 6) was identified in the in the Palaeocene deposits, from Frasin area, Eastern Carpathians, Romania.

Genus *Amphisphaera* Haeckel 1881, emend. Petrushevskaya 1975

Species *Amphisphaera coronata* Ehrenberg, 1873

Description.

This species has a small, subspherical outer shell with circular pores set in hexagonal frames. Two polar outer spines of different lengths. The largest spine is about the same length as the main axis of the

outer shell and is conical rather than cylindrical proximally and tapering abruptly distally. The spine is rarely more than a third the length of the main axis of the outer shell and is simply conical rather than cylindrical proximally and tapering abruptly distally (Bąk, & Barwicz-Piskorz., 2005et al., 2005).

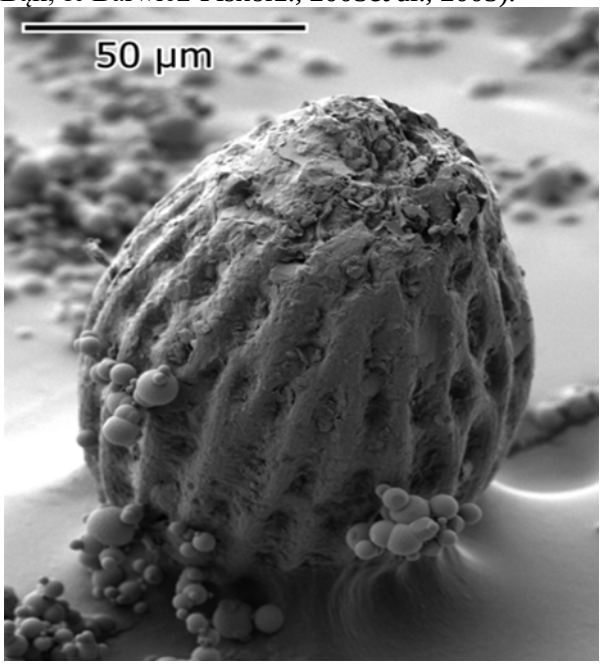

Figure 15. *Podocyrtis (Podocyrtis) papalis* (SEM photo).

The specimen (Fig. 16, Plates 3, 5) was identified in an outcrop from Frasin area, Eastern Carpathians, Romania. This species is distinguished from "*Stylosphaera*" *coronata coronata* by the length and shape of its shorter polar spine.

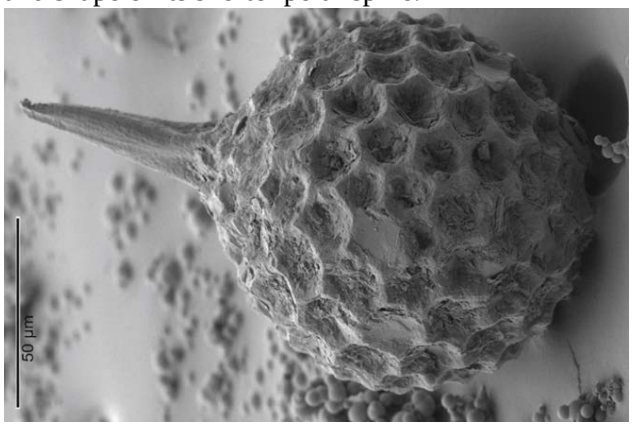

Figure 16. *Amphisphaera coronata* (SEM photo).

Ascidian Spicule

For the didemnid spicules, the 3-D reconstruction also helped in the determination process. We could precisely measure the rays on the both sides of its body, as well as the distance between them. We were also able to measure the diameter of the spicule body.

Family Didemnidae Giard, 1872

Description: The spherical spicule is 120 µm in diameter and it has conical to slightly rounded thirteen short rays, which seem to be symmetrically arranged. The transitional zone between the rays is slightly rough and the ratio between ray length and spicule diameter is 0.16.

Due to the lack of specific characteristics in these spicules, as well as the presence of similar sclerites in many different groups, it is difficult to assign these spicules to specific didemnid genera. The spicule (Fig. 17, Plates 3, 6) has been identified in the same middle Miocene deposits from Costești area, Republic of Moldova.

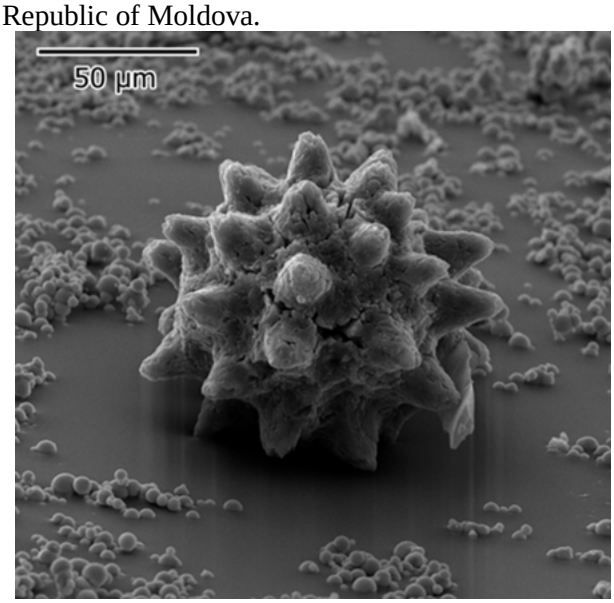

Figure 17. Didemnidae–like spicule (SEM photo).

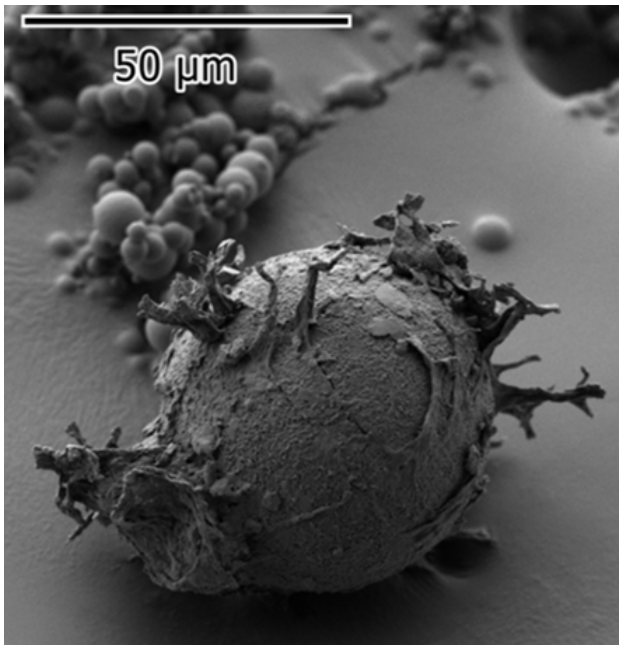

Figure 18. *Spiniferites bentorii pannonicus* (SEM photo).

Dinoflagellate cyst

In the case of the dinoflagellate cyst, the 3-D

reconstruction helped us to do a better determination. Using the 3-D models the processes were precisely measured on the both sides of the body of the cyst, as well as the distance between them. Also the diameter of the spicule body can be very easy calculated using this method.

Genus *Spiniferites* Mantell, 1850

Species *Spiniferites bentorii pannonicus* (Sütőné Szentai 1986)

Description. The specimen is a dinoflagellate cyst, with an oval shape, with the paratabulation clearly expressed by low ridges between the processes. The processes are hollow, relatively short, distally trifurcate or bifurcate. The periphragm is smooth to finely granulate.

The specimen (Fig. 18, Plates 3, 6) has been identified in the Middle Miocene deposits from Republic of Moldova.

4. CONCLUSIONS

Using the "Structure-from-Motion" method we managed to obtain a high quality 3-D model for different types of microfossils. Until now, for a better representation of the microfossils, SEM photos were used, from which we could only observe the elements from the angle that the specimen was photographed. In the best case scenario we would use stereo photos which would be viewed with 3-D glasses.

Following this study we consider that by using the "Structure-from-Motion" photogrammetry method high resolution 3-D models can be obtained for any microfossil, which later can be included in a common digital format such as a 3-D PDF.

This method can be successfully used on holotypes of the microfossils by orienting the specimen in advance, so that the 3-D reconstruction would capture the most important parts without the need to reorient it, as in the examples presented on the Methods chapter.

These 3-D models obtained through this method have other advantages as well. They have the same high resolution as the SEM photographs used in the reconstruction process, the amount of the detail being limited just by the performance of the electronic microscope and the number of photos taken.

High resolution 3-D models offer a realistic representation of the studied specimen. By adding textures to these models even more realism is achieved and the digital microfossil will help the observer in his study.

The size of the morphological elements, which are important for different types of species (the size of the spines, apertures, the distances between ribs or pores, the dimension of the pores, etc.), can be precisely measured directly on the model using any 3-D modelling software (in case of the original format of the 3-D models) or directly in the PDF interface (using the attached PDF plates). Using the same tools, the angles of different morphological elements (apical angle) as well as different morphological elements of the specimens (the angle between the dorsal margin and the posterior margin at the ostracods, the angle between the spine and the surface of a spicule, etc.) can also be easily measured.

Furthermore, using the 3-D model the surface of the specimen can be calculated. Using this calculations the roughness degree can be determined, by comparing the specimen with an ideal geometric body (sphere, cylinder, ellipsoid, cone, etc.)

Due to the fact that any point from the 3-D model is defined by a xyz coordinates system, any morphological element can be highlighted making it easier to identify it, thus adding precision to the morphometric method used in the microfossil study.
By using all the information extracted with the "Structure-from-Motion" method, we consider that any 3-D microfossil can be fully described in an accessible way.

Furthermore, a 3-D reconstruction using photogrammetry for the outer part of the fossil it is better in most of the cases than micro-computer tomography not only because of its cost, but also because it can create models for any type of microfossil, with sizes smaller than the microcomputer tomography limit of 50 μm.

Moreover, the resulting 3-D models can be shared between collaborating researchers (who may choose to 3-D print the specimen at a larger scale), therefore helping them to visualize in detail any specimen with its morphological features and texture, and allow anyone to perform any measurement at a distance, without the need to physically send any sample.

In addition, the reconstruction of the fossils in 3-D allows students to do individual study from their own computer and it offers them the possibility to examinate in detail a holotype without the risk of deteriorating the specimen.

Acknowledgments

Authors want to thank to POCU/380/6/13/123623 project for the financial support in publication of this paper. We are also thanking to Constantin Costea and Daniel Bîrgăoanu, from Geological Institute of Romania, Microcosmos laboratory, for their support in providing high quality SEM photos for some of our specimens. Also, the authors want to express their gratitude towards Nvidia Co. for their hardware support without whom the achievement of this paper would not have been possible.

PLATE 1

The pyrite 3-D reconstructed model

The separated tetrahedron from the pyrite model

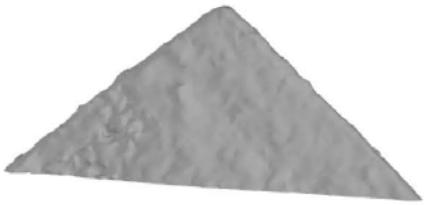

The 3-D tetrahedron created in sckethup

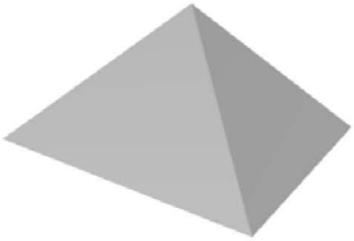

PLATE 2

Cycloforina karreri karreri

Quinqueloculina minakovae ukrainica

Cyprideis pannonica

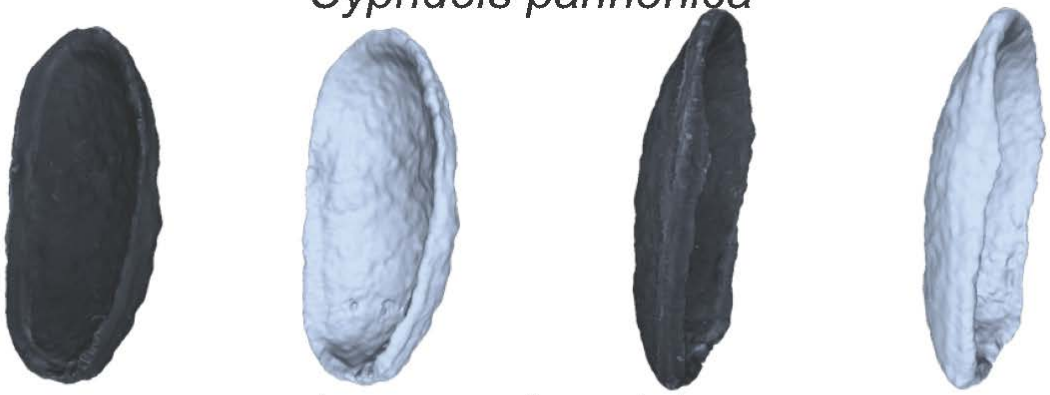

Loxoconcha minima

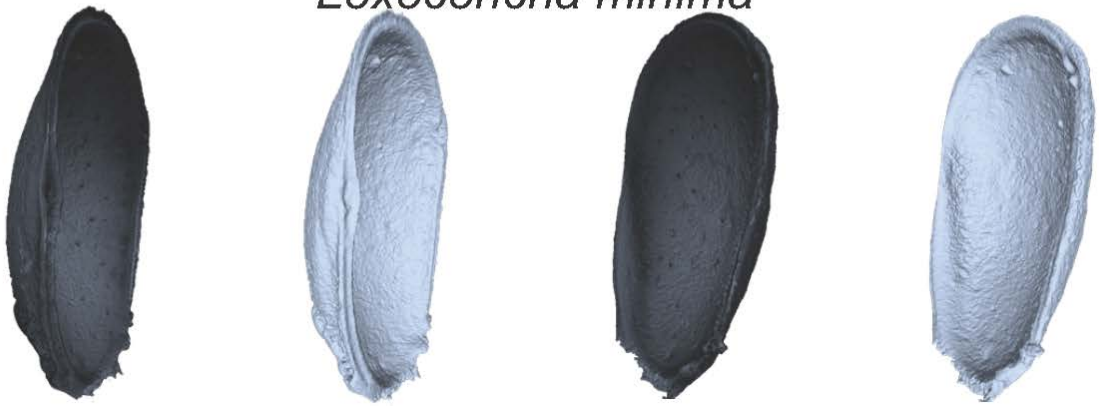

PLATE 3 *Amphisphaera coronata* (a and b)

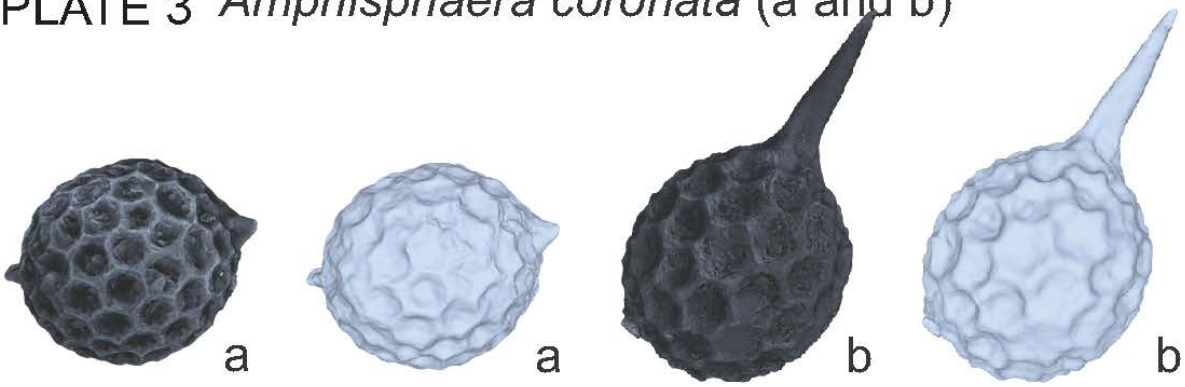

Podocyrtis (Podocyrtis) papalis

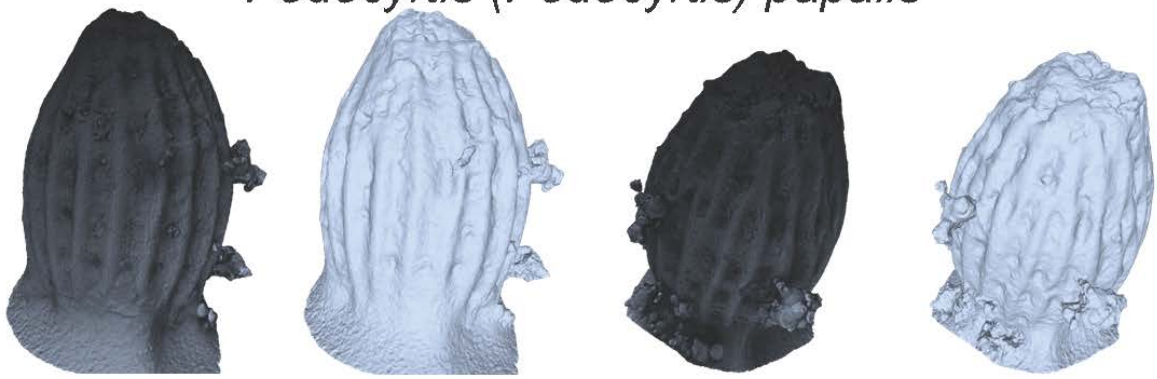

Spiniferites bentorii pannonicus

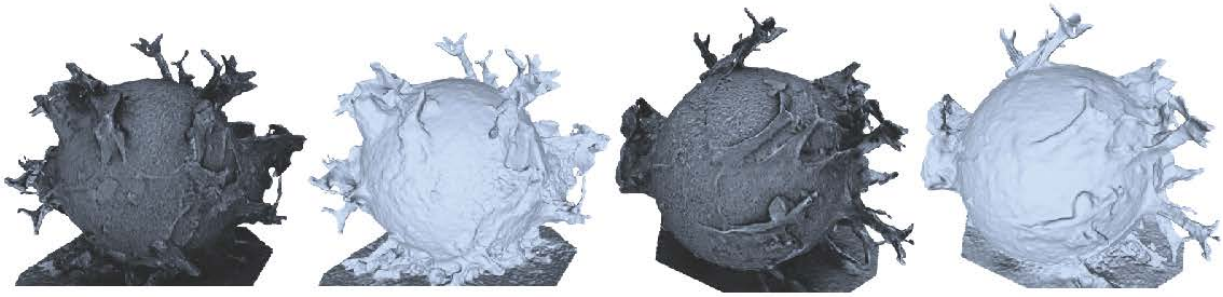

Didemnum – like spicule

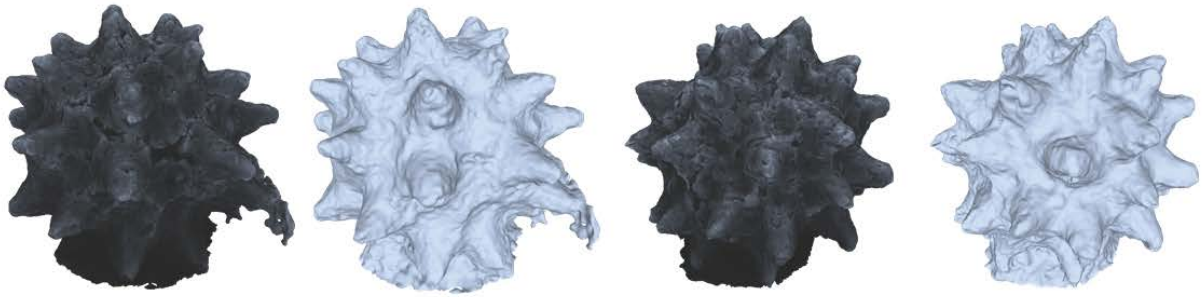

PLATE 4

Cycloforina karreri karreri

TEXTURED MESH

SIMPLE MESH

Quinqueloculina minakovae ukrainica

TEXTURED MESH

SIMPLE MESH

Cyprideis pannonica

TEXTURED MESH

SIMPLE MESH

PLATE 5 *Loxoconcha minima*

TEXTURED MESH

SIMPLE MESH

Amphisphaera coronate (a)

TEXTURED MESH

SIMPLE MESH

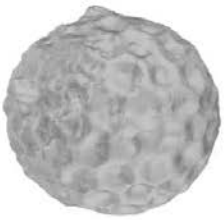

Amphisphaera coronata (b)

TEXTURED MESH

SIMPLE MESH

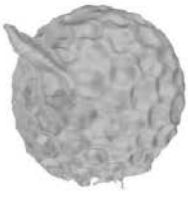

PLATE 6 *Podocyrtis (Podocyrtis) papalis*

TEXTURED MESH

SIMPLE MESH

Spiniferites bentorii pannonicus

TEXTURED MESH

SIMPLE MESH

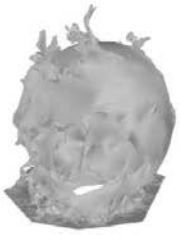

Didemnum - like spicule

TEXTURED MESH

SIMPLE MESH

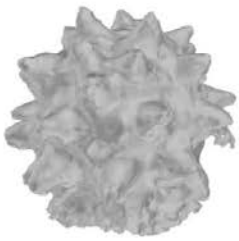

REFERENCES

Bąk, M. & Barwicz-Piskorz, W., 2005. *Stratigraphical and ecological significance of early Eocene radiolarians from the Subsilesian Series, Polish Flysch Carpathians.* Annales Societatis Geologorum Poloniae, 75, 139-153.

Bates, K.T., Breithaupt B.H., Falkingham, P.L., Matthews Neffra, A., Hodgetts, D. & Manning, P.L., 2009. *Integrated LiDAR & photogrammetric documentation of the Red Gulch Dinosaur Tracksite (Wyoming, USA).* In: **Foss, S.E., Cavin, J.L., Brown, T., Kirkland, J.I., and Santucci, V.L.** (Eds.), *Proceedings of the Eighth Conference on Fossil Resources*, Utah, pp. 101-103.

Belvedere, M., Baucon, A., Furin, S., Mietto, P., Felletti, F., & Muttoni, G., 2011. *The impact of the digital trend on ichnology: ICHNOBASE*. Dinosaur track Symposium Abstract Book, Obernkirchen, Germany.

Didkowski, V. I., 1961. *Miliolidi neogenovih pivdeno-zahidnoi ciastini roiskoi platform (Rodi: Quinqueloculina to Triloculina).* Gn. An. USRS, ser. stratigrafii to paleontologii, 39.

Dumitriu, T., C., 2013. *Towards digital preservation of Repedea's big quarry outcrop using "Structure-from-Motion" photogrammetry tools*. An. Șt. Univ. „Al. I. Cuza", Iași. 59 (2), 19-40.

Dumitriu, S. D., Dubicka, Z. & Ionesi, V., 2018. *The functional significance of the spinose keel structure of benthonic foraminifera: inferences from Miliolina cristata Millett, 1898 (Miliolida) from northeast Romania.* Journal of Micropalaeontology, 37: 153–166.

Ehrenberg, C.G., 1847. *Über die mikroskopischen kieselschaligen Polycystinen als mächtige Gebirgsmasse von Barbados und über das Verhältniss deraus mehr als 300 neuen Arten bestehenden ganz eigenthümlichen Formengruppe jener Felsmasse zu den jetzt lebenden Thieren und zur Kreidebildung. Eine neue Anregung zur Erforschung des Erdlebens.* K. Preuss. Akad. Wiss. Berlin, Ber., Jahre 1847:40–60.

Ehrenberg, C. G., 1873. *Grossere Felsproben des Polycystinen-Mergels von Barbados mit weiteren Erlauterungen. Monatsber*. K. Preuss. Akad. Wiss., Berlin, Jahrg., pp. 213-263.

Eulitz, M. & Reiss, G., 2015. *3D reconstruction of SEM images by use of optical photogrammetry software*. Journal of Structural Biology 191. 190–196.

Falkingham, P.L., 2012. *Acquisition of high resolution three-dimensional models using free, open-source, photogrammetric software.* Palaeontologia Electronica.

Gatesy, S.M., Bäker, M. & Hutchinson, J.R., 2009. *Constraint-Based exclusion of limb poses for reconstructing theropod dinosaur locomotion*. Journal of Vertebrate Paleontology, 29: 535-544.

Görög, A., Szinger, B., Tóth, E. & Viszkok, J., 2012. *Methodology of the micro-computer tomography on foraminifera*. Palaeontologia Electronica Vol. 15, Issue 1; 3T, 15p;

Gontard, L. C., Schierholz, R., Yu, S., Cintas, J. & Dunin-Borkowski, R. E., 2016. *Photogrammetry of the three-dimensional shape and texture of a nanoscale particle using scanning electron microscopy and freeware software, Ultramicroscopy*.

Giard, A. M., 1872. *Recherches sur les ascidies composees or synascidies*. Archives de zoologie experimentale et generale 1: 501–704.

Haeckel, E., 1881. *Entwurf eines Radiolarien-Systems auf Grund von Studien der Challenger-Radiolarien.* Jena. Z. Naturwiss. 15 (3), 25: 418-472.

Haynes, J.R., 1981. *Foraminifera.* Macmillan Publishers Limited, London, 443pp.

Hutchinson, J.R., Anderson, F.C., Blemker, S.S. & Delp, S.L., 2005. *Analysis of hindlimb muscle moment arms in Tyrannosaurus rex using a three-dimensional musculoskeletal computer model: implications for stance, gait, and speed.* Paleobiology, 31: 676-701.

Iglhaut, J., Cabo, C., Puliti, S., Piermattei, L., O'Connor, J. & Rosette, J., 2019. *Structure from Motion Photogrammetry in Forestry: a Review.* Current Forestry Reports, 5: 155-168.

Jones, T.R., 1857. *A monograph of the Tertiary Entomostraca of England*. Palaeontographical Soc. London, 68 pp.

Juad, M., Passot, S., Le Bivic, R., Delacourt, C., Grandjean, P. & Le Dantec, N., 2016. *Assessing the Accuracy of High Resolution Digital Surface Models Computed by PhotoScan and MicMac in Sub-Optimal Survey Conditions.* Remote Sensing, MDPI, 8 (6): pp.465.

Kitizato, H., 1988. *Locomotion of some benthic foraminifera in and on sediments*. Journal of Foraminiferal Research, 18 (4), 344-349.

Ling, H. Y., Hall, R. & Nichols, G. J., 1991. Journal of Southeast Asian Earth Sciences, Vol. 6, No. 3/4, pp. 299-305.

Loeblich, A.R., Jr. & Tappan, H., 1984. *Suprageneric classification of the Foraminiferida (Protozoa).* Micropaleon-tology, 30: 1–70.

Loeblich, A.R., Jr. & Tappan, H. 1987. *Some new and revised genera and families of hyaline calcareous Foraminiferida (Protozoa).* Transactions of the American Microscopical Society, 105: 239–265.

Łuczkowska, E. 1972. *Miliolidae (Foraminiferida) from Miocene of Poland, part I. Revision of the classification*. Acta Palaeontologica Polonica, 17 (3): 342–377.

Mantell, G.A., 1850. *A pictorial atlas of fossil remains, consisting of coloured illustrations selected from Parkinson's "Organic Remains of a Former World" and Artis's "Antediluvian Phytology*"- Bohn, London.

Méhes, G., 1908. *Beiträge zur Kenntnis der Pliozänen Ostrakoden Ungarns. II. Die Darwinulidaeen und Cytheridaeen der Unterpannonischen Stufe.*

Földtani Közlöny, 38 (7-10): 601-635.

Müller, G.W., 1894. *Die Ostracoden des Golfes von Neapel un d der angrenzeden Meeresabschnitte, Fauna und Flora des Golfes von Neapel.* Berlin, Monogr. 21, 404 p.

d'Orbigny, A. 1846. *Foraminiferes fossiles du bassin tertiaire de Vienne (Autriche).* Gide et Comp, Paris, XXXVII, 312 pp.

Petrushevskaya M. G., 1975. *Cenozoic radiolarians of the Antarctic, Leg 29, DSDP*. In: Kennett, J. P., Houtz, R. E., et al. Init. Repts. DSDP, 29: Washington (U.S. Govt. Printing Office), 541-675.

Reuss, A.E., 1869. *Zur fossilen Fauna der Oberoligocänschichten von Gaas*. Sitzungsberichte der Akademie der Wissenschaften in Wien, 59: 446-488.

Riedel, W.R. & Sanfilippo, A., 1970. *Radiolaria*, DSDP LEG 4, Initial Reports of the Deep Sea Drilling Project, 4, pp. 503-575. Washington, DC: US Government Printing Office.

Rybczynski, N., Tirabasso, A., Bloskie, P., Cuthbertson, R., & Holliday, C., 2008. *(Hadrosauridae) for testing chewing hypotheses.* Palaeontologia Electronica, 11.2.9A.

Sars, G.O., 1866. *Oversigt of Norges marine ostracoder. Förhandl. Vidensk.* Selskab Christiania 7: 1-130.

Sellers, W.I., Manning, P.L., Lyson, T., Stevens, K. & Margetts, L., 2009. *Virtual palaeontology: gait reconstruction of extinct vertebrates using high performance computing.* Palaeontologia Electronica, 12.3.13A,

Smith, N.E. & Strait, S.G., 2008. *PaleoView3D: from Specimen to Online Digital Model*. Palaeontologia Electronica.

Sütőné Szentai, M., 1986. *A magyarországi pannoniai s. l. rétegösszlet mikroplankton vizsgálata – Über das Microplankton mit Organischer Membranbildungen des Ungarischen Schichtenkomplex „Pannon s. l.„* – Folia comloensis 2: 25–45.

Sutton, M., Rahman, I. & Gardwoon, R., 2017. *Virtual paleontology – an overview*. The Paleontological Society Papers, 22: p. 1–20.

Van Morkoven, F.P.C.M., 1963. *Post-Palaeozoic ostracoda. Their morphology, taxonomy, and economic use. Volume 2*. Elsevier Publishing Company, Amsterdam - London - New York, 475pp.

Westoby, M.J., Brasington, J., Glasser, N.F., Hambrey, M.J. & Reynolds, J.M., 2012. *`Structure-from-Motion` photogrammetry: A low-cost, effective tool for geoscience applications.* Geomorphology, 179: 300-314.

Whatley, R.C., 1995. *Ostracoda and oceanic palaeoxygen levels.* Mitteilungen aus dem Hamburgischen Zoologischen Museum und Institut 92, 337–353.

Wynn, T., Petruny, L., Jett, J. & Whittaker, S., 2015. *Foraminifera photogrammetry: enhancing 3D modeling methods*. GSA Annual Meeting in Baltimore, Maryland, USA (1-4 November 2015). Paper No. 30-15.

Received at: 07. 10. 2020
Revised at: 16.01.2021
Accepted for publication at: 18. 01. 2021
Published online at: 25. 01. 2021